# An Inverse Modeling Approach to Assess the Impacts of Climate Change on Water Resources Management at the Watershed Scale

**Yoichi FUJIHARA**[1], **Slobodan P. SIMONOVIC**[2], **Fatih TOPALOGLU**[3], **Tsugihiro WATANABE**[4], **and Kenji TANAKA**[5]

[1,4]*Research Institute for Humanity and Nature, 457-4 Kamigamo-motoyama, Kita-Ku, Kyoto 603-8047*

[2]*Department of Civil and Environmental Engineering, University of Western Ontario, London, Ontario N6A 5B9, Canada*

[3]*Faculty of Agriculture, Cukurova University, Adana 01130, Turkey*

[5]*Disaster Prevention Research Institute, Kyoto University, Gokasho, Uji 611-0011*

## 1. Introduction

Over the last several years, hydrologists have paid great heed to the potential impacts of climatic change on water resources and hydrological cycling, which are traditionally assessed using a top-down approach. With this approach, outputs from general circulation models (GCMs) are statistically or dynamically downscaled to the river basin scale, and the local climatic signal is then input to a hydrological model to assess the direct consequences in the basin. However, problems related to this approach arise from the incompatibility between the temporal and spatial scales of a GCM and a river basin. Because serious effort is required to validate GCM outputs and the downscaling techniques, many river basin authorities consequently remain skeptical of the possible impacts of climate change.

We attempted to improve understanding of the processes leading to local hydrological hazards by introducing an inverse (or bottom-up) approach to the modeling of flood risk and vulnerability to changing climatic conditions. The modeling approach was applied to the Seyhan River Basin, Turkey.

## 2. Methods

The inverse modeling approach is designed to assess the vulnerability of river basin hydrological processes to climate forcing from a bottom-up perspective. The theoretical concepts of this approach were developed at the University of Western Ontario, Canada, by Cunderlik and Simonovic (2004, 2005, in press). The approach consists of the following four steps and is illustrated in **Figure 1**.

**1.** Critical hydrological exposures, which may lead to local failures of water resource systems in a particular basin, are first identified. Critical exposures are analyzed together with existing guidelines and management practices. This step is accomplished in collaboration with local water authorities.

**2.** In the next step, the identified critical hydrological exposures (such as floods and droughts) are transformed into corresponding critical meteorological conditions (e.g., extreme precipitation events, sudden warming, and prolonged dry spells). A hydrological model is used to establish the inverse link between hydrological and meteorological processes.

**3.** General circulation model (GCM) outputs are analyzed to investigate future changes relative to the present conditions. Afterward, a stochastic weather generator, which is one of the downscaling methods, is used to generate the meteorological conditions under present and future scenarios.

**4.** In the final stage, the frequencies of critical meteorological events causing specific water resources risks are assessed from the weather generator outputs. The frequencies of critical hydrological events are obtained using the established inverse link.

The presented approach can be used to develop hazard risk management strategies under present and future climatic conditions for any water resource system. The main advantages of the inverse

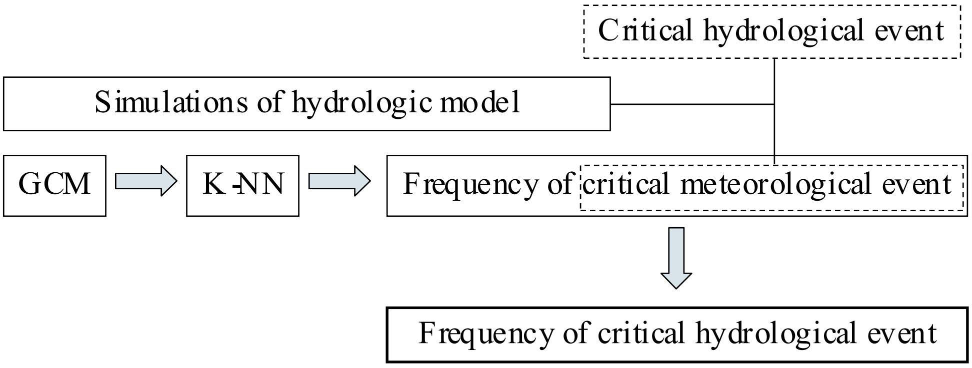


**Fig.1** The Framework of this Study

approach over the traditional top-down approach are its focus on specific existing water and potential water resource problems, a direct link with the end user, and easy updating when new and improved GCM outputs become available.

## 3. Results

### 3.1 Identification of Critical Hydrological Events

#### 3.1.1 Flood events

Adana, with a population of approximately 1.3 million, is the capital of Adana Province and the fourth largest city in Turkey. Socioeconomic activities in the lower area of the Seyhan River Basin are much more vital than those of the upper area. The urban center is located around and downstream from Seyhan Dam, which was constructed in 1956 to protect the city of Adana against floods.

The flood of 1980 was the biggest flood on record and also produced the most damage (Japan International Cooperation Agency, 1994). Flood damage occurred not only on the Cukurova Plain but also in upstream areas and around tributaries of the Seyhan River. Although the recently constructed Seyhan Dam was operating at the time, the flood of 1980 destroyed 21 buildings and damaged 76 others. The deluge was equivalent to a flood of 100-year probability.

The flood damage in 1980 accelerated the planning for and construction of the Catalan Dam. Dam construction began in 1982, and the Catalan Dam has been operating since 1997. The Catalan and Seyhan dams should be able to protect downstream areas against floods of 500-year probability. Based on these findings, 100-year and 500-year floods are identified as critical hydrological events in the Seyhan River Basin.

#### 3.1.2 Drought events

The Lower Seyhan Irrigation Project (LSIP) in Adana was initiated by the Turkish government as an important irrigation project covering an area of 204,000 ha. In 2002, approximately 1.8 $Gm^3$ of irrigation water was withdrawn from the Seyhan River for the LSIP. This withdrawal has increased annually, and region IV of the LSIP will be completed within several years. Therefore, water scarcity will be a major concern in the Seyhan River Basin. In this study, we employ the following index as a water scarcity index:

$$I_{ws} = \frac{W - S}{Q} \tag{1}$$

where $W$, $S$, and $Q$ are the annual water withdrawals by all sectors, use of desalinated water, and the annual inflow at Seyhan Dam, respectively. When this index is higher than 0.4, the Seyhan basin is considered highly water-stressed (Alcamo et al., 2003; Oki and Kanae, 2006). Drought, represented by a water scarcity index ($I_{ws}$) value higher than 0.4, is identified as a critical event in the Seyhan River Basin.

### 3.2 Hydrological Model Application

The simulation region is an area of 2.75° $\times$ 2.75° (36.5°-39.25° and 34.25°-37.0°) with 5 min latitude/longitude spatial resolution (33 $\times$ 33 grids). Gtopo30 was used as the digital elevation model (DEM). The Global Land Cover Characterization version 2.0 (GLCC-v2) was selected for the basic land use data. However, the irrigated

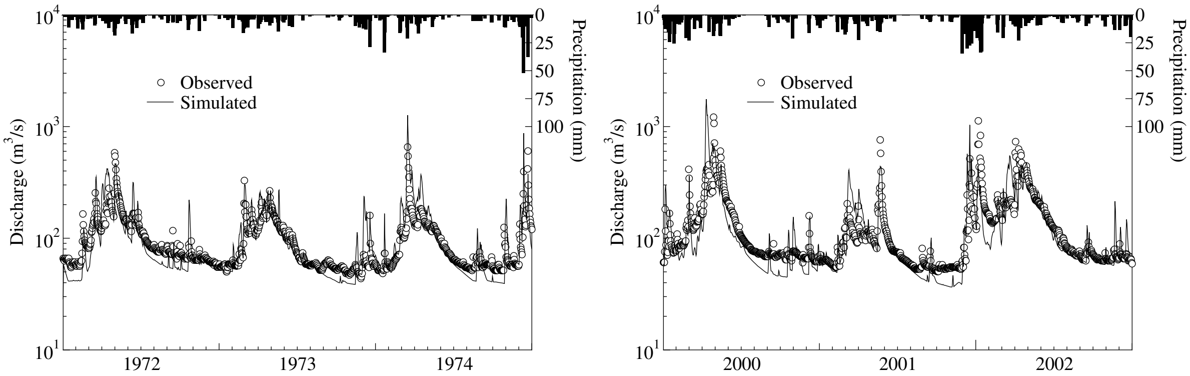


(a) 1972-1974 (b) 2000-2002

**Fig.2** Simulated Hydrograph at Station 1818

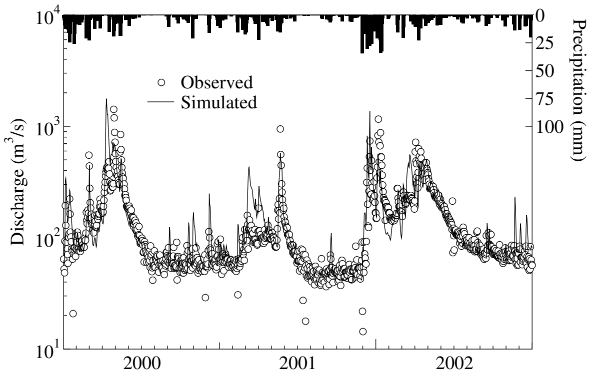


**Fig.3** Simulated Hydrograph at the Catalan Dam (2000-2002)

cropland and forest areas in the original data set are clearly underestimated. Thus, the data set was modified by ground truthing and normalized difference vegetation index (NDVI) time series analysis.

Grid precipitation and temperature data for Hydro-BEAM (Kojiri et al., 1998) were created by interpolating data from 23 stations. The inverse distance method (IDM) was employed as the spatial interpolation method. Hydro-BEAM was then run using the grid meteorological data from 1972 to 2002 to calibrate the model parameters. The simulated hydrographs at station 1818 for the first and last 3 years are shown in **Figure 2**. These figures show that the river discharge at station 1818 was quite well reproduced by Hydro-BEAM. Moreover, the simulated hydrographs at the Catalan Dam for the last 3 years are shown in **Figure 3**. This figure also shows that the simulated result agreed with the observed data.

### 3.3 Inverse Linkage

#### 3.3.1 Flood event

The 12 biggest floods from the historical record were selected as the representative flood events in the Seyhan River Basin. Analyzing the relationship between these floods and meteorological conditions, daily areal precipitation had a large influence on the floods. The inverse link between floods and areal precipitation was determined by the following procedures.

We created a synthetic precipitation data set to establish the relationship between the peak discharge and areal precipitation. Synthetic areal precipitation data sets (50, 100, 150, and 200 mm day$^{-1}$) were created by multiplying the ratio between observed areal precipitation corresponding to the flood event and the synthetic areal precipitation. Hydro-BEAM was run using each synthetic precipitation data value. **Figure 4** shows the relationship between the peak discharge and areal precipitation. After the average of peak discharge for each synthetic precipitation was obtained, the inverse linkage was established as follows:

$$Q = aP^2 + bP + c \quad (2)$$

where $Q$ is the peak discharge at the Catalan Dam, $P$ is the areal precipitation, and $a$, $b$, and $c$ are parameters.

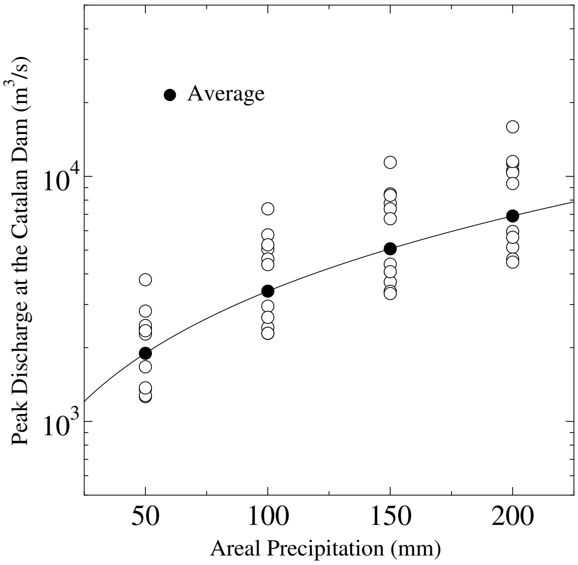


**Fig.4** Inverse Link (Peak Discharge)

### 3.3.2 Drought event

In this study, the water scarcity index ($I_{ws}$) was used as the index of drought. An advance analysis revealed that the water scarcity index can be approximated by areal annual precipitation. The inverse link between water scarcity and areal annual precipitation was obtained by the following procedures.

Data for all years were used to establish the relationship between the water scarcity index and areal annual precipitation. To create synthetic data in which the annual precipitation was set to half the value of the original data, we multiplied by 0.5. Hydro-BEAM was then run for the data of all years and the synthetic data. **Figure 5** illustrates the relationship between the water scarcity index and areal annual precipitation. The inverse linkage was obtained as follows:

$$I_{ws} = \exp(aP + b) \quad (3)$$

where $I_{ws}$ is the water scarcity index for a year, $P$ is the areal annual precipitation, and $a$ and $b$ are parameters.

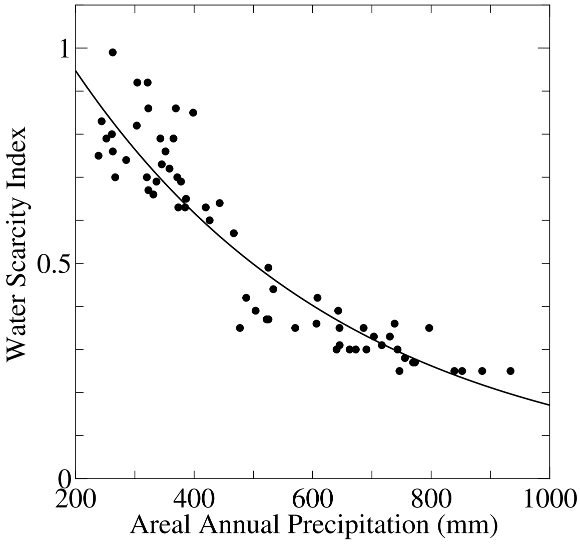


**Fig.5** Inverse Link (Water Scarcity Index)

### 3.3.3 GCM Projections

This study employed nine state-of-the-art GCMs that were also used in the most recent phase of the Coupled Model Intercomparison Project (CMIP; Covey et al., 2003). From the atmospheric data set, monthly precipitation and monthly mean temperature data under IPCC SRES A2 scenario were collected for each model. Two subset periods (present: 1961-1990 and future: 2070-2099) were set to investigate the temperature and precipitation changes.

**Figure 6(a)** indicates the ensemble averaged annual temperature of the nine GCMs, which project the rising annual temperatures in all regions; **Figure 6(b)** shows the ensemble averaged annual precipitation of the nine GCMs, which project the decreasing annual precipitation in the Mediterranean region, including Turkey. The decreasing precipitation and rising temperature predicted for the Mediterranean region suggest that climate change will have serious impacts on the hydrology and water resources of the Seyhan River Basin. We set the decreasing precipitation scenario for the weather generator based on these GCM analyses.

## 3.4 Frequency of Critical Hydrological Events

We adopted a modified version of the k-nearest neighbor approach (Sharif and Burn, 2004, 2006), which is one of the stochastic weather generators. The k-nn approach was applied to gener-

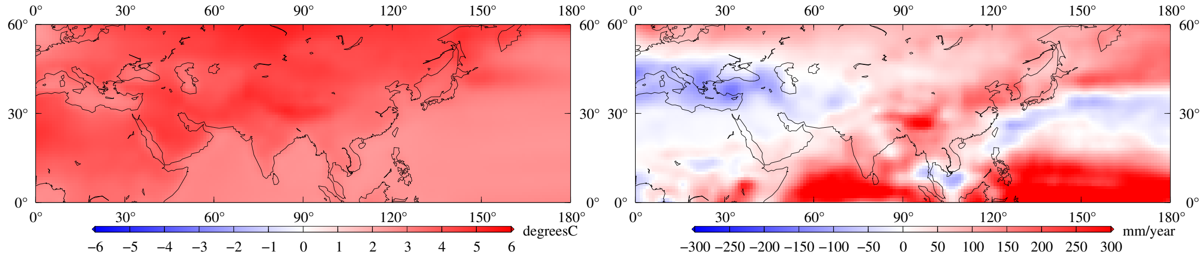


(a) Temperature (b) Precipitation

**Fig.6** Temperature and Precipitation Changes

ate the meteorological conditions corresponding to the scenarios (decreased precipitation) for a 100-year period. The frequency of critical meteorological events causing flooding was assessed from the weather generator outputs. The flood return periods, which were inversely estimated using equation (2), are shown in **Figure 7**. For 100-year flood, the future peak discharge is almost the same as that at present. However, the 500-year flood under present conditions will decrease to a flood of 250-year magnitude under the decreasing precipitation conditions. Thus, critical flood events will occur less frequently under the decreasing precipitation scenario.

The frequency of critical meteorological events causing drought was also assessed from the weather generator outputs. The return periods, which were inversely estimated using equation (3), are shown in **Figure 8**. Drought, indicated by $I_{ws}$ higher than 0.4, has about a 6-year probability under present conditions. However, the decreasing precipitation scenario indicates that droughts will occur more often, at a 2-year probability.

## 4. Conclusions

This study introduced an inverse bottom-up approach to the modeling of flood and drought risk under changing climatic conditions. The approach is focused on specific extant water resource problems, has a direct link with end-users, and can be easily updated when new and improved GCM outputs become available because the analysis of GCM outputs is the last step in the proposed methodology.

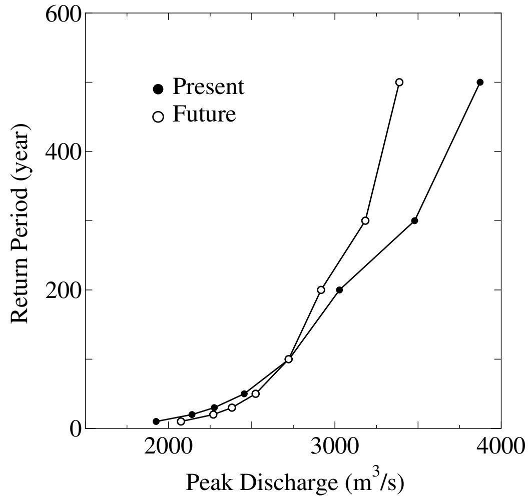


**Fig.7** Return Period (Peak Discharge)

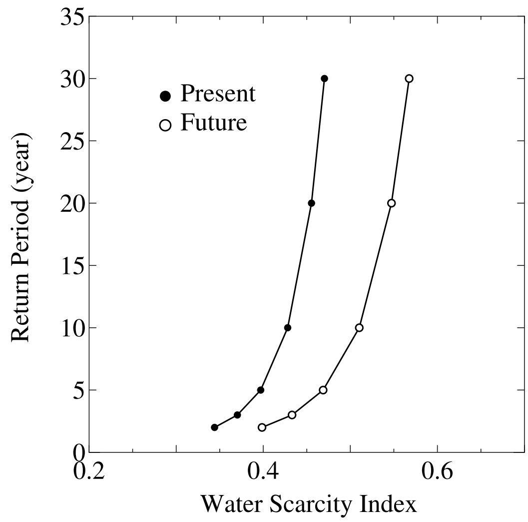


**Fig.8** Return Period (Water Scarcity Index)

The study case presented one possible application through its assessment of flood and drought risk in the Seyhan River Basin, Turkey, under present and future climatic conditions. Based on data and reports for the Seyhan River Basin, 100-year and 500-year floods were identified as critical hydrological events. In addition, drought, indicated by $I_{ws}$ higher than 0.4, was identified as a critical event in the Seyhan River Basin. The identified critical floods and drought were transformed into corresponding critical meteorological conditions using a Hydro-BEAM simulation. Based on analysis of the outputs of nine state-of-the-art GCMs, the decreased precipitation scenario was set for the weather generator. The k-nn was then used to generate meteorological conditions corresponding to the scenario for a 100-year period. The frequencies of critical meteorological events causing flooding and drought were assessed from the weather generator outputs. The frequency of flood and drought were then estimated using the established inverse link. The results suggest that the 500-year return period flood under the present condition will decrease to a 250-year return period flood under the decreasing precipitation conditions. Drought, with 6-year probability under the present condition, has 2-year probability under the future condition.

**Acknowledgments**

This research was supported financially by the Project Impact of Climate Changes on Agricultural Production System in Arid Areas (ICCAP), administered by the Research Institute for Humanity and Nature (RIHN) and the Scientific and Technical Research Council of Turkey (TUBITAK). In addition, this research was also supported financially in part by Japan Society for the Promotion of Science (JSPS) Grant-in-Aid No. 16380164.

## References

Alcamo, J., P. Doll, T. Henrichs, F. Kaspar, B. Lehner, T. Rosch, and S. Siebert (2003) Global estimates of water withdrawals and availability under current and future business-as-usual conditions, Hydrological Sciences Journal, 48(3), 339-348.

Covey, C., K.M. Achuta Rao, U. Cubasch, P. Jones, S.J. Lambert, M.E. Mann, T.J. Phillips, and K.E. Taylor (2003) An overview of results from the Coupled Model Intercomparison Project (CMIP), Global and Planetary Change, 37, 103-133.

Cunderlik, J.M., and S.P. Simonovic (2004) Inverse modeling of water resources risk and vulnerability to changing climatic conditions, Proceedings of the 57th CWRA Annual Congress, Water and climate change: Knowledge for better adaptation, 16-18 June, Montreal, Canada.

Cunderlik, J.M., and S.P. Simonovic (2005) Hydrological extremes in a southwestern Ontario river basin under future climate conditions, Journal of Hydrologic Sciences, 50(4), 631-654.

Cunderlik, J.M., and S.P. Simonovic (in press) Inverse flood risk modeling under changing climatic conditions, Hydrological Processes.

Japan International Cooperation Agency (1994) Feasibility study on flood control, forecasting and warning system for Seyhan River Basin, 5-6.

Kojiri, T., A. Tokai, and Y. Kinai (1998) Assessment of river basin environment though simulation with water quality and quantity, Annuals of Disaster Prevention Research Institute, Kyoto University, 41(B-2), 119-134.

Oki, T., and S. Kanae (2006) Global hydrological cycles and world water resources, Science, 313, 1068-1072.

Sharif, M., and D.H. Burn (2004) Development and application of k-nearest neighbor weather generating model, Proceedings of the 57th CWRA Annual Congress, Water and climate change: Knowledge for better adaptation, 16-18 June, Montreal, Canada.

Sharif, M., and D.H. Burn (2006) Simulating climate change scenarios using an improved k-nearest neighbor model, Journal of Hydrology, 325, 179-196.